Accepted Manuscript

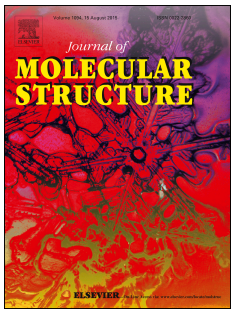

Crystal, Hirshfeld, ADMET, drug-like and anticancer study of some newly synthesized imidazopyridine containing pyrazoline derivatives

Sharanya Kuthyala, Manjuanatha Hanumanthappa, S. Madan Kumar, Sana Sheik, Nagaraja Gundibasappa Karikannar, Ashwini Prabhu

PII: S0022-2860(19)30865-8

DOI: https://doi.org/10.1016/j.molstruc.2019.07.031

Reference: MOLSTR 26784

To appear in: *Journal of Molecular Structure*

Received Date: 9 April 2019

Revised Date: 20 June 2019

Accepted Date: 5 July 2019

Please cite this article as: S. Kuthyala, M. Hanumanthappa, S. Madan Kumar, S. Sheik, N. Gundibasappa Karikannar, A. Prabhu, Crystal, Hirshfeld, ADMET, drug-like and anticancer study of some newly synthesized imidazopyridine containing pyrazoline derivatives, *Journal of Molecular Structure* (2019), doi: https://doi.org/10.1016/j.molstruc.2019.07.031.

This is a PDF file of an unedited manuscript that has been accepted for publication. As a service to our customers we are providing this early version of the manuscript. The manuscript will undergo copyediting, typesetting, and review of the resulting proof before it is published in its final form. Please note that during the production process errors may be discovered which could affect the content, and all legal disclaimers that apply to the journal pertain.

Graphicl Abstarct

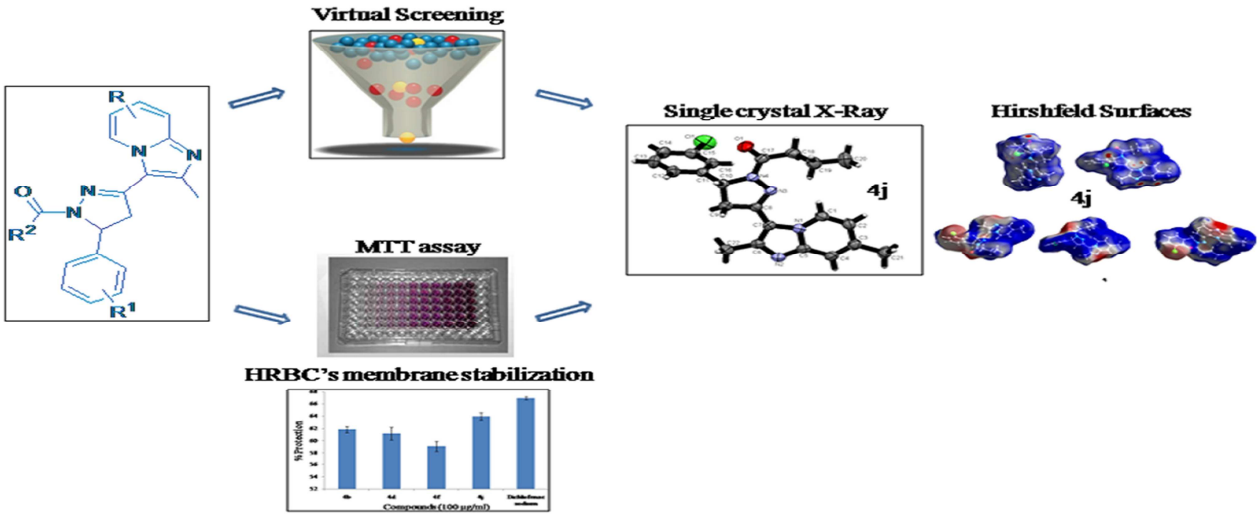

ACCEPTED MA

ACCEPTED MANUSCRIPT

Crystal, Hirshfeld, ADMET, drug-like and anticancer study of some newly synthesized imidazopyridine containing pyrazoline derivatives

Sharanya Kuthyala [a], Manjuanatha Hanumanthappa [b], Madan Kumar S [c], Sana Sheik [d], Gundibasappa Karikannar Nagaraja *, Ashwini Prabhu [e].

[a] *Department of Chemistry, Mangalore University, Mangalagangothri, Karnataka, India,*
[b] *Department of Biotechnology Kuvempu University Shankaraghatta, Shimoga, Karnataka, India,*
[c] *DST-PURSE Lab, Mangalore University, Mangalagangothri, Karantaka, India.*
[d] *Department of Botany, St. Aloysius College, Mangalore, Karnataka, India,*
[e] *Yenepoya Research centre, Yenepoya (Deemed to be university), Deralakatte, Mangalore, Karnataka, India*

Abstract

To steer the selection of a potent drug, computer models have been fostered as a valid alternative to reduce pharmacokinetics related failure. The present study mainly focuses on the relationship between molecular properties and anticancerous activity of some newly synthesized aza heterocycles. Twelve new imidazo[1,2-a]pyridine incorporated pyrazoline derivatives were synthesized and were well characterized by ^{1}HNMR, ^{13}CNMR, LC-MS analysis. X-ray study resolved the structure of 4g, 4i and 4j as monoclinic crystal system. To quantify the electrostatic potential distribution and percentage intermolecular contacts in crystal packing, Hirshfeld surface study was performed. Moreover, virtual screening focused on ADMET and drug-like attributes to identify a promising derivative among the series. The anticancerous activity of the compounds was evaluated against A549 cell line. The study was further validated by subjecting best active compounds to induced hemolysis, which finally confirmed 4j as a potent molecule both in computational and *in vitro* study.

Keywords: Imidazopyridine-pyrazoline; X-Ray; Hirshfeld; ADMET; Anticancer; Hemocompatibility.

1. Introduction

Cancer burden is rapidly increasing across the globe. The world health organization is estimating that globally almost one in six deaths are caused by this disease, which has led to around 9.6 million deaths in 2018 [1]. It is one with highest levels of attrition due to the failure of potential anticancer drug entering clinical development and challenge for a successful drug is still making its way over multiple

hurdles. Virtually, the statistics are rather bleak in terms of potential drug to tackle the causes that are fueling cancer [2].

The heterocycles are so ubiquitous in medicinal chemistry, their unique physicochemical property and intrinsic versatility, have poised them as a key structural component of many anticancerous drugs available in the market today [3]. In addition, defined with dual mode of action, the hybrid molecule strategy can lead to powerful therapeutics in current advances [4], as they are capable of functioning as one single molecule, thus minimizing the drug resistance and lowering the drug-drug interaction.

Recently, imidazopyridine, a fused heterocycle is featuring as Drug Prejudice prominently in the field of medicinal chemistry [5]. Their prevalence in the field is, due to their various therapeutic properties including anticancerous, anti-inflammatory, analagesics, anxiolytic, antiviral [6, 7] etc. It is also a core structure of many of the established drugs such as zolpidem, nicopidem, alpidem, fadrazole, olpinone, rifaximin, zolmidine, saripidine etc. [8]. Many studies have reported the anticancer activity of certain imiazopyridines and their different mode of action but it is important to reduce the dose to the least extent possible in order to minimize the undesirable toxic effects on the test system. Besides, diversely substituted pyrazolines with variety of functional groups have contributed significantly in the field of drug discovery. Many new compounds have been introduced as antimicrobial [9], anticancerous [10] anti-inflammatory, analgesic [11, 12], antidepressant [13] etc and many patented [14]. It is precisely reported that pyrazolines are not only useful in various types of cancer treatment but also have the ability to act as cancer chemopreventive agents [15]. Given all of this, in the current work we targeted the integration of imidazopyridine and pyrazoline in a single molecule as hybrid.

Molecular shapes or Hirshfeld surface analysis (HS) plays important role in understanding chemistry and biochemistry. This study represents the boundaries of a molecule in the crystalline environment and interprets electron density distributions and crystalline interactions [16, 17]. This HS is associated with properties like d_i (distance to the nearest internal atom) and d_e (distance to the nearest

external atom) and d_{norm} (distance between internal and external atoms normalized by Vander Waals radii, thus visualizes the fidelity of the crystal structure.

To detect the safer and potential drug candidate ADMET profile has been fostered for the early stage estimation of parameters in the discovery process. These computer models have constituted a valid alternative in time and resource-consuming process of drug discovery and developments. Thus, *in silico* study enables a key to access pharmacokinetic, physicochemical and other drug-like parameters for one or more molecules with fast predictive models [18, 19].

2. Results and Discussion

2.1. Chemistry

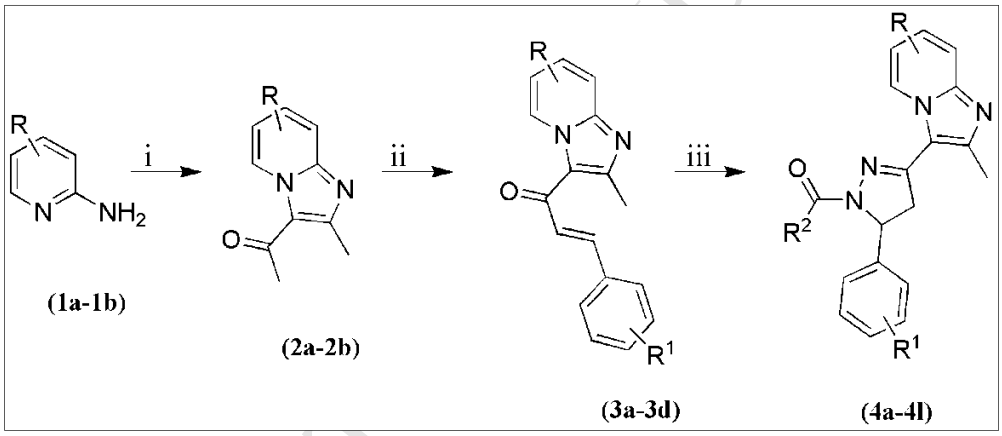

Scheme 1. : i) 3-Chloro-2, 4-pentadione, DCM, reflux, 4h; ii) -2OH/-3Cl Benzaldehyde, ethanol, 40% NaOH, RT, 24 h; iii) $NH_2NH_2.H_2O$, Acetic/Propionic/Butyric acid, reflux, 8 h.

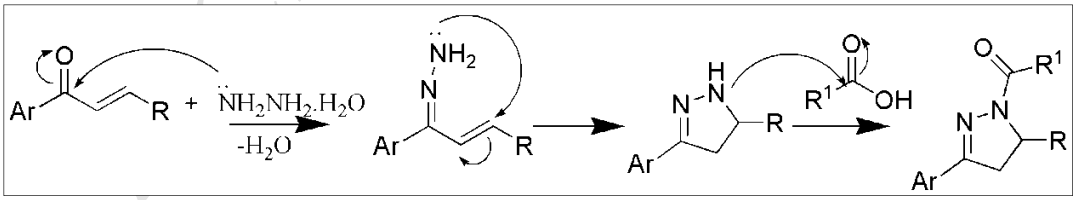

Fig. 1. Mechanism of pyrazoline formation.

Synthetic route and mechanism for the objective compounds are shown in Scheme 1 and Fig. 1. As depicted, the synthesis of intermediate (3a-3d) was achieved in two steps [4], further cyclization with the hydrazine hydrate in the presence of excess acetic/propionic/butyric acid gave the targeted hybrid

molecules (4a-4l) in good yield (Table 1). The structures of all the synthesized compounds were analyzed by FT-IR, ^{1}HNMR, ^{13}CNMR, LC-MS spectroscopy.

Sample Code	R	R^1	R^2	Molecular formula	Molecular weight	% Yield	Melting point (^{0}C)
4a	4-CH_3-pyr	2-OH-C_6H_5	CH_3CO-	$C_{20}H_{20}N_4O_2$	348.3984	69	238-240
4b	4-CH_3-pyr	3-Cl-C_6H_5	CH_3CO-	$C_{20}H_{19}ClN_4O$	366.8440	72	186-188
4c	5-CH_3-pyr	2-OH-C_6H_5	CH_3CO-	$C_{20}H_{20}N_4O_2$	348.3984	73	290-292
4d	5-CH_3-pyr	3-Cl-C_6H_5	CH_3CO-	$C_{20}H_{19}ClN_4O$	366.8440	72	208-210
4e	4-CH_3-pyr	2-OH-C_6H_5	CH_3CH_2CO-	$C_{21}H_{22}N_4O_2$	362.4642	65	148-150
4f	4-CH_3-pyr	3-Cl-C_6H_5	CH_3CH_2CO-	$C_{21}H_{21}ClN_4O$	380.8706	67	162-164
4g	5-CH_3-pyr	2-OH-C_6H_5	CH_3CH_2CO-	$C_{21}H_{22}N_4O_2$	362.4642	66	234-236
4h	5-CH_3-pyr	3-Cl-C_6H_5	CH_3CH_2CO-	$C_{21}H_{21}ClN_4O$	380.8706	66	154-156
4i	4-CH_3-pyr	2-OH-C_6H_5	$CH_3CH_2CH_2CO$-	$C_{22}H_{24}N_4O_2$	376.4515	79	124-126
4j	4-CH_3-pyr	-3-Cl-C_6H_5	$CH_3CH_2CH_2CO$-	$C_{22}H_{23}ClN_4O$	394.8972	78	220-222
4k	5-CH_3-pyr	2-OH-C_6H_5	$CH_3CH_2CH_2CO$-	$C_{22}H_{24}N_4O_2$	376.4515	79	128-130
4l	5-CH_3-pyr	3-Cl-C_6H_5	$CH_3CH_2CH_2CO$-	$C_{22}H_{23}ClN_4O$	394.8972	79	156-158

Table 1. Physical data of imidazopyridine-pyrazoline hybrid molecules.

The FT-IR spectrum, manifested the presence of characteristic bands for O-H, C-H, C=O, C=C and C=N group. The bands for 4a were observed at 3130, 2931, 1641, 1581 and 1456 cm^{-1} respectively. In ^{1}HNMR spectrum (Fig.2) signal for acetyl-CH_3, pyridine-CH_3 and imidazole-CH_3 protons resonated as a singlet at 2.381, 2.417 and 2.472 ppm respectively. H_A proton resonated at 3.106 ppm as a doublet of doublet with coupling constant J_{AB} = 17.2 Hz and J_{AX} = 4.4 Hz. Similarly H_B and H_X appeared as doublet of doublet at 4.017 and 5.581 ppm with the coupling constants J_{BA} = 17.2 Hz & J_{BX} = 12 Hz and J_{XA} = 4.4 Hz & J_{XB} = 11.6 Hz respectively. Among the aromatic protons, the signal for 2- hydroxyphenyl-5H appeared at 6.704 ppm as a triplet with coupling constant *J*=7.6 Hz. The 2-hydroxyphenyl-6H proton resonated at 6.834 ppm as a doublet with coupling constant 8 Hz. At 6.890 ppm, a doublet appeared for 2-hydroxyphenyl-3H with *J*= 7.6 Hz. A singlet for imidazopyridine-9H was found at 7.424 ppm and a doublet at 9.294 with *J* value 6.8 Hz was observed for imidazopyridine-6H. Phenolic-OH proton resonated at 9.744 ppm as a singlet and remaining two aromatic protons resonated as multiplets at 7.031-7.092 ppm respectively.. In ^{13}CNMR, peaks for three methyl groups appeared at 15.7 ppm (acetyl-CH_3),

20.7 ppm (pyr-CH_3) and 21.9 ppm (imid-CH_3) respectively. All other characteristic peaks were within 43.1-166.9 ppm. LC-MS showed molecular ion peak at 349.80 (M+1) (Fig. 3).

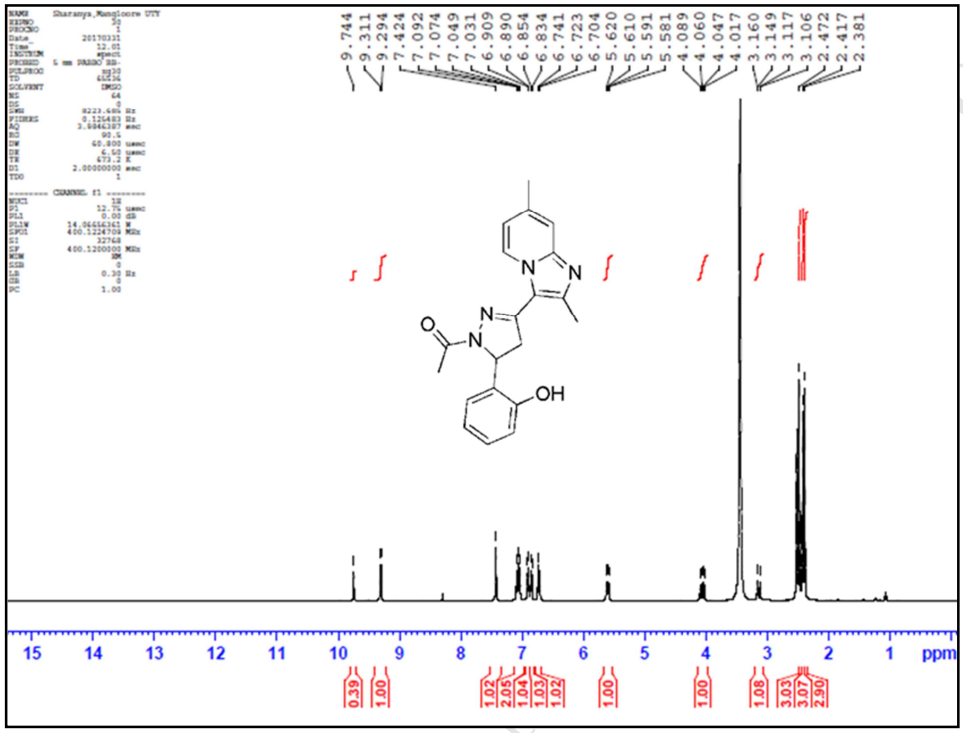

Fig 2. ^{1}HNMR of 4a.

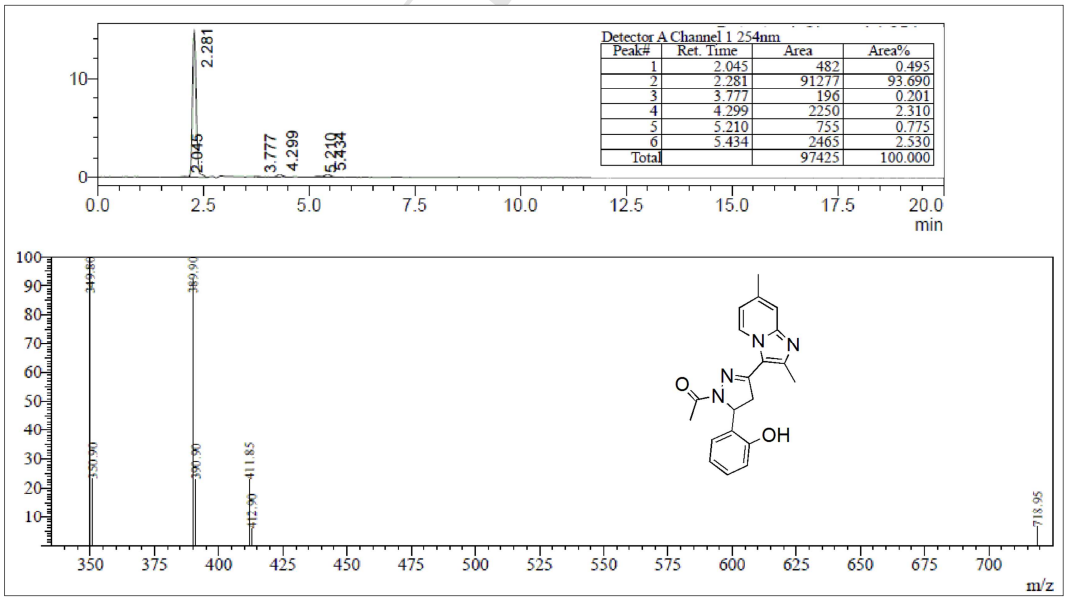

Fig. 3. LC-MS of 4a.

2.2. Single crystal X-Ray crystallography study

The proposed molecular structure for the compound **4g, 4i** and **4j** were confirmed by the single crystal XRD studies and are shown in Fig. 4. In the unit cell of the compound 4g, two molecules were crystallized with solvent molecules (water and ethanol). The dihedral angles between pyrazole (Cg6/Cg2:N3A/B-N4A/B-C10A/B-C12A/B) and phenyl rings (Cg8/Cg4:C13A/B-C18A/B) in molecule A and molecule B were $77.76(15)^0$ and $87.56(17)^0$ respectively. The crystal structure was stabilized *via* intermolecular hydrogen bonds (O---H...O, O---H...N, C---H...O) and intermolecular interactions (C---H...π and π...π). The Cg1...Cg7: Cg3 N1B/C2B-C3B/C5B-C7B)...Cg7 and Cg6...Cg8 (C13A-C18A) exists with a distance of 3.6758 (17), 3.6167 (16) and 3.7514(16) respectively.

The compound 4i crystallizes with butyric acid solvent. The dihedral angle between Cg1 (N1-N2/C7-C9) and Cg4 (C1-C6) is 73.8(3)°. Intramolecular hydrogen bonds of the type C---H…N were observed. The crystal structure was stabilized through intermolecular hydrogen bonds (O--- H…O), intermolecular interactions (C---H…π) and π...π interactions between Cg2 (N3/C10/C11/N4/C13)…Cg2 (3.570 Å, symmetry 1-X,1-Y,1-Z).

In the crystal structure of 4j, the Cg2 (N3-N4/C8-C10) makes dihedral angles of $77.16(12)^0$ (C11-C16) and $18.17(10)^0$ (N1/C1-C5/N2-C6-C7), with Cg4 and Cg5, respectively. The dihedral angle between Cg4 and Cg5 is $80.25(10)^0$ and intramolecular hydrogen bonds C---H...N were observed. The crystal structure was stabilized *via* intermolecular hydrogen bonds (C---H...O and C---H...N) and intermolecular interactions (C---H...π and π...π) (Fig.4.). The Cg2...Cg4: exists with a distance of 3.7669 (14) Å.

Parameters	**4g**	**4i**	**4j**
CCDC number	1568088	1889128	1587575
Empirical formula	$2(C_{21}H_{22}N_4O_2)$, H_2O, C_2H_6O	$(C_{22}H_{24}N_4O_2)0.5$, $(C_4H_7O_2)0.5$	$C_{22}H_{23}ClN_4O$
Formula weight	788.93	231.27	394.89
Temperature	293(2) K	293(2)	293(2) K
Wavelength	0.71075 Å	0.71075 Å	0.71075 Å

Crystal system, space group	monoclinic, $P2_1/n$	monoclinic, *I2/a*	monoclinic, $P2_1/c$
Unit cell dimensions	*a* = 12.2407(6) Å *b* = 14.4681(8) Å *c* = 23.9361(11) Å β = 92.701(4) º	*a* = 15.3022(16) *b* = 16.2017(14) *c* = 20.3832(17) β = 100.025(10)	*a* =8.5348(6) Å *b*=29.9913(14) Å *c* = 8.8956(7) Å β = 115.865(9) º
Volume	4234.4(4) $Å^3$	4976.3(8) $Å^3$	2048.9(3) $Å^3$
Z, Calculated density	4, 1.238 Mg/m^3	16,1.237 Mg/m^3	4, 1.280 Mg/m^3
Absorption coefficient	0.084 mm^{-1}	0.085 mm^{-1}	0.206 mm^{-1}
$F_{(000)}$	1680	1976	832
Crystal size	0.21x0.23x0.24 mm	0.17 x 0.23 x 0.27 mm	0.25 x0.32x+0.41 mm
Theta range for data collection	1.7º to 25.7°	2.5 º to 25.0 º	2.6º to 25.0°
Limiting indices	-14≤ h ≤ 14, -17 ≤ k ≤ 17, -29≤ l ≤29	-14 ≤ h ≤ 18, -19≤ k ≤ 19,-24 ≤ l ≤ 24	-10≤ h ≤ 10, -35 ≤ k ≤ 35, -10≤ l ≤10
Reflections collected / unique	44905/8031 [R(int) = 0.068]	25151/4388 [R(int) = 0.105]	20789/3609 [R(int) = 0.048]
R - value	0.0694	0.0965 (0.2669)	0.0492
Refinement method	Full-matrix least-squares on F^2	Full-matrix least-squares on	Full-matrix least-squares on F^2
Data / restraints / parameters	4948 / 0 / 547	$F^2$4388 / 0 / 316	2875 / 0 / 256
Goodness-of-fit on F^2	1.04	1.04	1.04
Largest diff. peak and hole	0.23 and−0.22. $Å^{-3}$	0.24 and −0.25	0.29 and −0.32. $Å^{-3}$

Table 2. Crystal structure and refinement parameters.

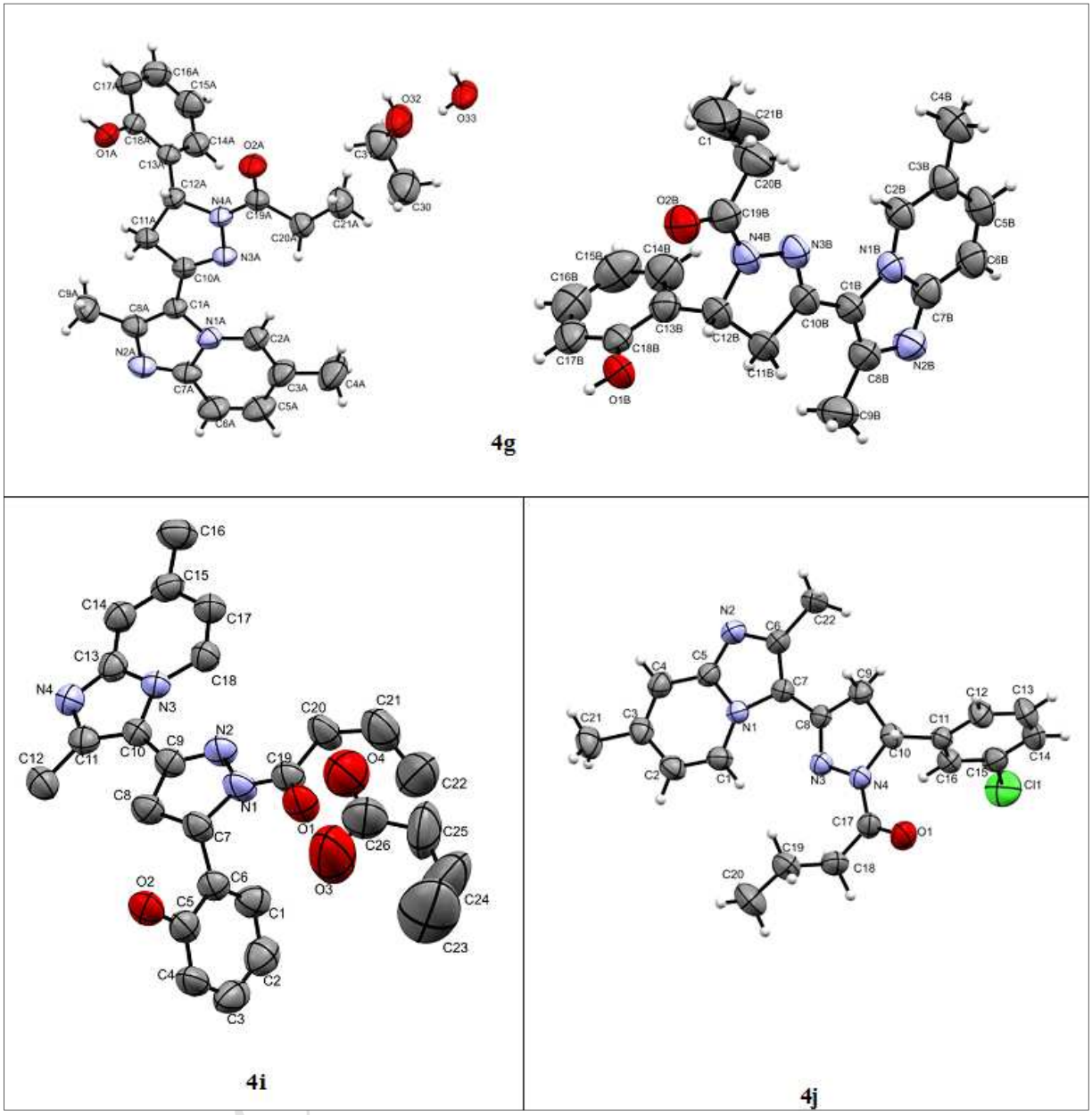

Fig. 4. ORTEP of 4g, 4i and 4j.

2.3. Hirshfeld analysis

A graphical tool 'Hirshfeld surfaces computational method' was assessed, to explore and visualize the intercontacts within the crystal lattice [20]. Conventional mapping of d_{norm} on molecular Hirshfeld surfaces were highlighted and given in supplementary and Fig. 5 for 4g and 4j respectively. Also the percentages of intercontacts were calculated and the 2D- finger print plots shown in the

supplementary details and Fig.5. The compound **4g** exhibits; C…C (2.8%), C…H (16.69 %), H…H (60.1 %), H…N (5.9 %), N…C (2.7 %), O…H (11.4 %) and other interactions in molecule A. In molecule B, C…C (2.6%), C…H (16.3%), H…H (58.7%), H…N (6.2%), N…C (2.7%), O…H (12.8%) and other interaction were the major interactions observed. In the associated ethanol molecule mainly H…N (7.8%), H…H (78.8%) and O…H (12.7%) with other interaction were found and C…H (3.2%), H…N (10.8%), O…H (40.1%) and H…H (45.7%) were observed in associated water molecule respectively. The intercontacts C…C (1.3%), C…Cl (2.4%), C…H (17.9%), Cl…H (8.8%), Cl…N (1.4%), H…H (51.3%), N…H (8.8%), O…H (74%) with other interactions were observed for **4j. A**lso the electrostatic potential was mapped using wave function STO-3G basis set at Hatree-Fock theory over the range of ±0.030 au and are given in supplementary details and Fig.5 [5]. The hydrogen donor potential is represented by blue region, which indicates positive electrostatic potential, where as the negative electrostatic potential (hydrogen bond acceptor) is visualized by red region.

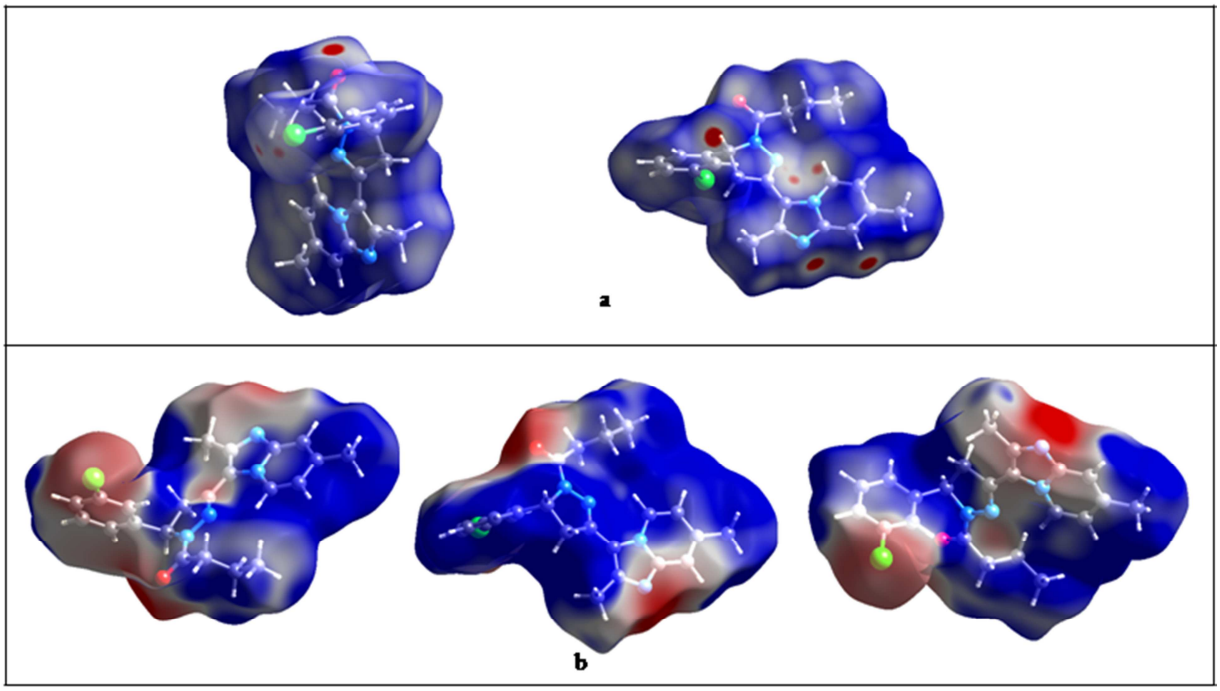

Fig.5. a. Hirshfeld surfaces and their corresponding 2D finger print plots for the compound 4j; b. Electrostatic potential mapped on Hirshfeld surface (different orientations) with +-20 au. Red regions correspond to negative electrostatic potential and blue region corresponds to positive electrostatic potential.

2.4. ADMET prediction

Predicted ADMET score has been tabulated in Table 3. Absorptivity efficacy of all 12 derivatives were found to be very good (96.17-99.61%) via human intestinal tract. In addition they have shown medium permeability in Caco-2 cell model, Madin-Darbg Canine Kidney (MDCK) model and Blood Brain Barrier (BBB) Model. The pharmacodynamic behaviour of drug depends on uptake and distribution, can possibly be ascertained by Plasma Protein Binding. Here the molecules have shown medium binding affinity. Also, the toxicity prediction score, the carcinogenic and mutagenic effects of pyrazoline derivatives were evaluated. All the compounds except 4i exhibited negative results to mouse toxicity.

Comp.	HIA (%)	BBB (%)	Caco2 (nm/sec)	MDCK (nm/sec)	PPB (%)	Ames test	Mouse toxicity
4a	96.17	0.3604	28.30	21.96	80.40	Mutagen	Negative
4b	97.51	1.296	38.35	123.38	90.38	Mutagen	Negative
4c	96.17	0.2618	29.11	41.76	80.38	Mutagen	Negative
4d	97.51	1.8250	38.36	79.92	90.13	Mutagen	Negative
4e	96.19	0.3281	32.43	2.287	87.06	Mutagen	Negative
4f	97.56	1.0342	41.22	27.39	91.22	Mutagen	Negative
4g	96.19	0.2496	33.06	30.51	86.91	Mutagen	Negative
4h	99.61	0.6967	55.43	7.827	91.49	Mutagen	Negative
4i	96.22	0.2970	35.22	0.9392	88.33	Mutagen	Positive
4j	97.61	0.7791	43.83	26.82	91.00	Mutagen	Negative
4k	96.22	0.2467	35.87	8.378	88.19	Mutagen	Negative
4l	97.61	1.1975	43.83	8.695	90.82	Mutagen	Negative

*****Classification: (% HIA): 0-20 % (poorly absorbed) 20-70 % (moderately absorbed), 70-100 % (well absorbed); BBB: > 1(CNS active), < 1 (CNS inactive); Caco-2 cell permeability: < 4 (low permeability), 4-70 (medium permeability), > 70 (higher permeability); MDCK: < 25 (low permeability), 25-500 (medium permeability), > (higher permeability); plasma protein binding: > 90 (strongly bound), < 90 (weakly bound).

Table 3. ADMET Property Evaluation.

2.5 Drug-like prediction study

The concept of drug ability involves consideration of how chemical properties compare with those approved drug to reduce the failure in clinical trials. Drug-like score has been tabulated in Table 4. The number of rotatable bonds in 4i to **4j** molecules is found to be 4 indicating more flexibility than 4a to 4h molecules (2 to 3). All molecules are having nitrogen bonding ability in the range from 5 to 6, while

the molecules 4a, 4c, 4e, 4g, 4i and 4k are showing single hydrogen bonding ability and the remaining molecules are having no hydrogen bonding property. Hydrogen and nitrogen bonding ability of all molecules has been directly related to TPSA property, where we found parallel increased value of 4a, 4c, 4e, 4g, 4i and 4k molecules (70.21) indicating higher TPSA property of those molecules, whose H and N bonding ability is more. Lipophilicity (milog P) is important property, which influences oral availability of the molecules. The miLogp of 4f, 4h, 4i, **4j**, 4k and 4l molecules lies in the range 4.64 to 5.20, indicating higher lipophilicity compared to 4a to 4e and 4g molecules (3.09 to 3.90). However, two molecules (**4j** and 4l) are having highest 5.20 value (≤ 5). Interestingly, milogp value proportionately increased with increased volume of these molecules showing drug-like property.

Compound	MW	miLogP	TPSA	nON	nOHNH	nrotb	Volume
4a	348.41	3.09	70.21	6	1	2	316.17
4b	366.85	3.80	49.98	5	0	2	321.69
4c	348.41	3.09	70.21	6	1	2	316.17
4d	366.85	3.80	49.98	5	0	2	321.69
4e	362.43	3.93	70.21	6	1	3	332.97
4f	380.88	4.64	49.98	5	0	3	338.49
4g	362.43	3.93	70.21	6	1	3	332.97
4h	380.88	4.64	49.98	5	0	3	338.49
4i	376.46	4.49	70.21	6	1	4	349.77
4j	394.91	5.20	49.98	5	0	4	355.29
4k	376.46	4.49	70.21	6	1	4	349.77
4l	394.91	5.20	49.98	5	0	4	355.29

Table 4: Drug likeness score for compounds.

2.6. Anticancer study

Among the series of novel imidazopyridine hybrid derivatives tested, the compounds 4b, 4f, **4j** and 4d were found to possess significant anticancer activity with IC_{50} values of 43.56, 53.35, **44.49** and 48.52 µM respectively, against A549 lung adenocarcinoma cells. Increase in the cytotoxicity was found to be concentration-dependent with these test compounds. IC_{50} values of the test compounds on A549 cells are represented in Table 5. Cisplatin was used as a standard drug, which showed an IC_{50} value of 14.87 µM. Thus compounds 4b and **4j** may be considered as a promising effective compound for further validations.

Compound	Cytotoxicity	IC_{50} (µM)

	(100µM, mean % ± SD)	
4a	2.08±0.31	-
4b	**80.30±0.61**	**43.56**
4c	0.79±0.19	-
4d	**77.09±0.69**	**48.52**
4e	3.33±0.40	-
4f	**71.17±0.71**	**53.35**
4g	58.82±1.14	-
4h	34.89±0.87	-
4i	13.64±0.57	-
4j	**85.31±0.71**	**44.49**
4k	8.63±1.73	-
4l	41.26±0.23	-

Table 5. Cytotoxicity of the compounds (4a-4l) on A549 cellline.

2.7. *HRBC's membrane stabilization*

The prevention of hypotonicity induced human erythrocyte membrane lysis was assessed and expressed as percentage protection. Thus the extent of inhibition against haemolysis was taken as a measure of anti-inflammatory activity. The compounds at its 100 µg/mL concentration showed 59-63 % protection as compared with 66.9% protection produced by the Diclofenac at same concentration (Fig. 6), where **4j** was found to be most active with 63% protection.

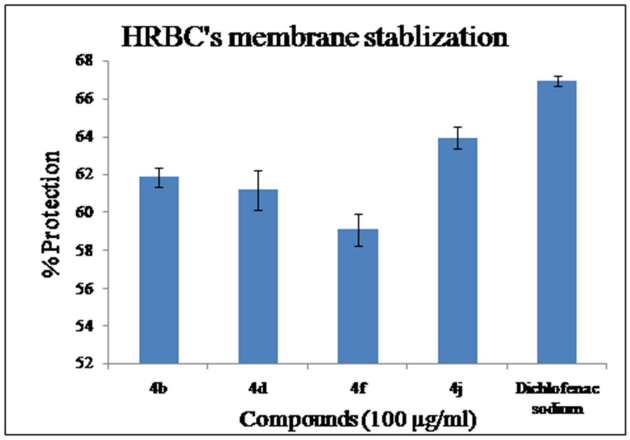

Fig. 6. Percentage HRBC's membrane stabilization of 4b, 4d, 4f and 4j.

3. Experiments

3.1 Materials and methods

All the required chemicals were purchased from Spectrochem India and Sigma Aldrich. These were used without any further purification. To check progress of the reaction Thin Layer Chromatography plate-aluminium sheet was used which was coated with Silicagel $60F_{254}$. These were visualized by UV light. Melting point was determined by open capillary method and it was uncorrected. ^{1}HNMR and ^{13}CNMR spectra were recorded on Bruker Avance III, 400MHz and Bruker Ascend, 400 MHz respectively using DMSO as solvent. The IR spectrum was analysed on Bruker Alpha spectrometer, LC-MS was carried out on Schimadzu LCMS-8030. The X-ray intensity data was collected at 296 K on a Rigaku Saturn724 diffractometer using graphite monochromated Mo-Kα radiation.

3.3 General procedure for the synthesis of 4a-4l

The mixture of imidazopyridine-chalcone **3a-3d** (0.01mol), hydrazine hydrate (0.01mol) in excess of acetic/ propionic/butyric acid was heated under reflux for 6 hours. The reaction mixture was cooled; the solid product formed was filtered, washed with cold water and recrystallized using suitable solvent mixture.

3.2. Single crystal X-Ray crystallography study

Good quality crystals of 4g, 4i and 4j were grown in dimethylformamide solvent by slow evaporation of the solvent at room temperature. The asymmetric unit of the title compounds is given in Fig. 4. The crystal parameters and data refinement are given in the Table 2. The detailed specification about software and steps followed are given in supplementary details. The structure was solved by direct methods and refined by full-matrix least squares method on F^2. Detailed account on structure refinement of all the three crystals has been included in supplementary details.

3.3. Hirshfeld analysis

The intermolecular interactions within the crystal structure are quantified and visualized using Hirshfeld surfaces computational method [21, 22, 23, 24]. The percentages of intercontacts are calculated

and the 2D- finger print plots are shown in the figure. The Hirshfeld surfaces are highlighted by conventional mapping of d_{norm} on molecular Hirshfeld surfaces.

3.4. ADMET prediction

The ADMET (Absorption, Distribution, Metabolism, Excretion and Toxicity) is pre-requisite in drug design and discovery studies since the attributes of the molecules play a critical role in pre-clinical and clinical phase. PreADMET property is a web-based application software used to predict ADMET (http://preadmet.bmdrc.kr/) of (4a to 4l) pyrazole derivatives. Further details are given in supplementary details.

3.5. Drug-like Prediction study.

The concept of drug ability involves consideration of how chemical properties compare with those approved drug to reduce the failure in clinical trials. In the present work, the molecular properties and bioactivity of imidazopyridine derivatives (4a to 4l) was evaluated using Molinspiration cheminformatics server (http:// www.molinspiration.com/). The server has wide range of tools for the dispensation and manipulation of molecules including generation of molecule fragmentation, tautomerization, normalization, calculation of various molecular properties needed in QSAR (Quantitative Structure Activity Relationship) study such as molecular descriptors, selection of training test etc., also supports fragment and crystal based virtual screening. In addition, the server calculates the molecular properties based on Lipinski/ Pfizer's Rule of five (RO5) [25] to evaluate drug-like study that would make it a likely orally active predicting bioactivity score for the most important therapeutic targets like GPCR receptor kinase inhibitors, ion channel modulators, enzymes and nuclear receptors [26].

3.6. Anticancerous Study

Cytotoxicity of the compounds on A549 cells was evaluated using MTT assay [27], the details are given in supplementary details.

3.7. HRBCs membrane stability assay

The membrane stability assay was performed by slight modified method of Padmanabhan and Jangle [28]. The detailed steps followed are discussed in supplementary details.

Conclusion

Herein we report a concise approach to synthesize a hybrid system containing imidazopyridine and pyrazoline scaffolds. It was successfully characterized by FT-IR, ^{1}HMR, ^{13}CNMR, LC-MS and single crystal XRD techniques. Hirshfeld surface analysis visualized the electrostatic potential distribution and intermolecular close contacts in crystal packing. Through virtual screening 4b, 4d, 4f, 4h, **4j** and 4l found to be with good ADMET properties. Whereas, **4j** and 4l showed good lipophilicity character. Further, from MTT assay, 4b and **4j** ascertained good anticancerous activity on A549 cell line. Additionally, hemocompatibilty study validated the compound **4j** with very good membrane stabilizing property. Thus results of the present investigation reveals an insight into the possibility of developing **4j** as potential chemotherapeutic agents for lung cancer, after appropriate validation with pre-clinical and clinical studies.

Acknowledgement

Authors are grateful to DST-PURSE-Mangalore University; STIC-Cochin, Kerala; MIT-Manipal. Karnataka for providing spectroscopy analysis.

Reference

[1] www.who.int/news-room/fct-sheets/details/cancer.

[2] http://labblog.uofmhealth.org/industry-dx/why-so-many-promising-new-cancer-drugs-fail-clinical-trials.

[3] http:// www.ddw-online.com/therapeutic/p320375-the -imoortance-of-heterocyclic-compounds-in-anti-cancer-drug-design.html.

ACCEPTED MANUSCRIPT

[4] S. Kuthyala, G. K. Nagaraja, S. Sheik, M. Hanumanthappa, M. S. Kumar, Synthesis of imidazo[1,2-a]pyridine-chlacones as potent inhibitors against A549 cell line and their crystal studies, J. Mol. Struct. 1177 (2019) 381-390.

[5] S. Kuthyala, M. K. Shankar, G. K. Nagaraja, Synthesis, single crystal X-Ray, Hirshfeld and antimicrobial evaluation of some new imidazopyridine nucleus, Chemistryselect, 3 (2018) 12894-12899.

[6] Y. Dabiri, R. A. Gawa-Bambika, K. Taskova, K. Herold, S. Reuter, J. Adjaye, J. Uttikal, R. Mrowka, J. Wang, M. A. Androde-Navarro, X. Chang, Imidazopyridine as potent KDM5 Demethylase Inhibitors promoting reprogramming efficiency of human iPSCs, iScience, 12 (2019) 168-181.

[7] H. Hosseini, M. Bayat, An efficient synthesis of new imidazo[1,2-a]pyridine-6-carbohydrazide and pyrido[1,2-a]pyrimidine-7-carbohydrazide derivatives via a five component cascade reaction, RSC Adv., 9 (2019) 7218-7227.

[8] D. Singh, G. Kumar, D. Dheer, Jyoti, M. kushwaha, Q. N. Ahmed and R. Shankar, BCl3-Mediated C−N, C−S, and C−O Bond Formation of Imidazo[1,2-a]pyridine Benzylic Ethers, ACS Omega, 4 (2019), 4530-4539.

[9] A. V. Chate, A. A. Relawar, G. M. Bondle, A.P. Sarkate, S. V. Tiwari, D. K. Lokwanid, A new efficient domino approach for the synthesis of coumarin-pyrazolines as antimicrobial agents targeting bacterial D-alanine-D-alanine ligase, New J. Chem., 43 (2019), 9002-9011.

[10] D. C. Liu, M. J. Gao, Q. Huo, T. Ma, Y. Wang, C. Z. Wu, Design, synthesis, and apoptosis-promoting effect evaluation of novel pyrazole with benzo[d]thiazole derivatives containing aminoguanidine units, J. **Enzyme** Inhib. Med. Chem., 34 (2019) 829-837.

[11] M. F. El Shehrya,d , E. F. Ewiesb, E. M. Zayedc, Synthesis of New Pyrazole Derivatives, Their Anti-Inflammatory and Analgesic Activities, and Molecular Docking Studies, Russ. J. Gen. Chem. 89 (2019) 492-498.

[12] V. Shivapura, Dinesha, P. S. Khandige, G. K. nagaraja, S. Ballav, S. S. Kerkar, Design and synthesis of some new pyrazolyl-pyrazlines as potent anti-inflammatory, analgesic and antibacterial agents, Eur. J. Med. Chem. 101 (2015) 442-451.

[13] A. C. Tripathi, S. Upadhyay, S. Paliwal, S. K. Saref, N1-benzene sulfonyl-2-pyrazoline hybrids in neurological disorders: Synthesis, biological screening and computational studies, EXCLIJ. 17 (2018) 126-148.

[14] S. Kumar, S. Bawa, S. Drabu, R. Kumar, H. Gupta, Biological activities of pyrazoline derivatives-A recent development, Recent Pat. Antiinfect. Dug Discov. 4 (2009) 154-163.

[15] M. Karbacak, M. D. Altmtop, H. I. Ciftvi, R. Koga, M. Ostuka, M. Fujita, A. Qzdemir, Synthesis and evaluation of new pyrazoline derivatives as potential anticancer agents, Molecules, 20 (2015) 19066-19084.

[16] C. Villa-Pérez, I. C. Ortega, A. Vélez-Macías, A. M. Payán, G. A. Echeverría, D. B. Soria, G. C. Valencia-Uribe, Crystal Structure, Physicochemical Properties, Hirshfeld Surface Analysis and Antibacterial Activity Assays of Transition Metal Complexes of 6-Methoxyquinoline, New J. Chem., 42 (2018), 7166-7176.

[17] M. F. Zaini, I. A. Razak, M. Z. Anis, S. Arshad, Crystal structure, Hirshfeld surface analysis and DFT studies of (E)-1-(4-bromophenyl)-3-(3-fluorophenyl)prop-2-en-1-one, Act. Cryst. E., 75 (2019), 58-63.

[18] O. A. Yousif, M. F. Mahdi, A. R. Raauf, Design, synthesis, preliminary pharmacological evaluation, molecular docking and ADME studies of some new pyrazoline, isoxazoline and pyrimidine derivatives bearing nabumetone moiety targeting cyclooxygenase enzyme, J. Contemp. Med. Sci. 5 (2019) 41-50.

[19] A. Diana, O. Michielin, V. Zoete, SwissADME: a free web tool to evaluate pharmacokinetics, rug-likeness and medicinal chemistry friendliness of small molecules, Sci. Rep.7 (2017) 1-13.

ACCEPTED MANUSCRIPT

ACCEPTED MANUSCRIPT

[20] P. R. Speckman, S. P. Thomas, D. Jayatilaka, High throughout profiling of molecular shapes in Crystals, Sci. Rep. 6 (2016) 1-9.

[21] S. K. Wolff, D. J. Grimwood, J. J. McKinnon, D. Jayati-laka, M. A. Spackamn, Crystal Explorer 3.0 Uni-versity of Westren Australia, Perth, 2007.

[22] M. A. Spackman, J. J. Mckinnon, Fingerprinting intermolecular interactions in molecular crystals, Cryst. Eng. Comm**.** 4 (2002), 378-392.

[23] S. M. Kumar, B. C. Manjunath, G. S. Lingaraju, M. M. M. Abdoh, M. P. Sadashiva, N. K. Lokanath, A Hirshfeld Surface Analysis and Crystal Structure of 2'-[1-(2-Fluoro-Phenyl)-1H-tetrazol-5-Yl]-4-Methoxy- Biphenyl-2-Carbaldehyde, Crystal Structure Theory and Applications, Cryst. Struct. Theory Appl. 2 (2013**)**, 124-131.

[24] M. A. Spackman, J. J. Mckinnon, D. Jayatilaka, Electrostatic Potentials Mapped on Hirshfeld Surfaces Provide Direct Insight into Intermolecular Interactions in Crystals, *Cryst*. Eng. Comm. 10 (2008**)**, 377-388.

[45] C. A. Lipinski, Lead- and Drug-like Compounds: the rule-of-fve evolution. Drug Discov. Today Technol. 1 (2004) 337–341.

[26] P. Ertl, B. Rohde, P. Selzer, Fast calculation of molecular polar surface area as a sum of fragment-based contributions and its application to the prediction of drug transport properties. J. Med. Chem. 43 (2000) 3714–3717.

[27] T. Mosmann, Rapid colorimetric assay for cellular growth and survival: application to proliferation and cytotoxicity assays. J. Immunol. Methods, 65 (1983) 55-63.

[28] Padmanabhan, Jangle., Evaluation of *in vitro* anti-inflammatory activity of herbal preparation, a combination of four medicinal plants, Int. J. App. Basic Med. Res. 2 (2012), 109-116.

ACCEPTED MANUSCRIPT

Highlights

- New imidazopyridine-pyrazolines were synthesized and well characterized.
- Crystal structures of 4g, 4i and 4j were well defined and analyzed their Hirhsfeld surfaces.
- Virtual screening predicted ADMET property, Druglike and bioactivity scores.
- Anticancerous activity against A549 was evaluated and validated by docking study.
- HRBCs membrane stabilization property of most active compounds was evaluated.

ACCEPTED MANUSCRIPT